Relative-phase ambiguities in measurements of ultrashort pulses with well-separated multiple frequency components

Dorine Keusters and Howe-Siang Tan

Department of Chemistry and the Center for Ultrafast Laser Applications, Princeton University, Princeton, New Jersey 08544

Patrick O'Shea, Erik Zeek, and Rick Trebino

School of Physics, Georgia Institute of Technology, Atlanta, Georgia 30332

Warren S. Warren

Department of Chemistry and the Center for Ultrafast Laser Applications, Princeton University, Princeton, New Jersey 08544

Received January 3, 2003; revised manuscript received April 25, 2003

Ultrashort-pulse characterization techniques, such as the numerous variants of frequency-resolved optical gating (FROG) and spectral phase interferometry for direct electric-field reconstruction, fail to fully determine the relative phases of well-separated frequency components. If well-separated frequency components are also well separated in time, the cross-correlation variants (e.g., XFROG) succeed, but only if short, well-characterized gate pulses are used. © 2003 Optical Society of America

OCIS codes: 320.7100, 320.5540.

1. INTRODUCTION

The past decade has seen great progress in the complementary fields of femtosecond shaped-pulse generation[1,2] and shaped-pulse measurement.[3–6] The most common pulse-shaping methods, which operate in the frequency domain, can independently modulate more than 1000 different frequency components, potentially yielding highly complex pulses. Even without such modulation methods, pulses with high complexity arise naturally as the result of some physical processes, such as continuum generation. Fortunately, pulse-shape detection methods have also evolved greatly in recent years, and pulses of very great complexity (time–bandwidth product >1000) were recently characterized.[7]

Traditional measurement methods, such as taking the autocorrelation and the pulse spectrum, give only a gross approximation of the generated pulse shape. Measurement of time–frequency profiles, first proposed by Treacy[8] and others, provided a large step forward. The approach was dramatically simplified with the introduction of self-referenced techniques, such as that of Chilla and Martínez[9] and frequency-resolved optical gating (FROG) with its algorithms to extract the pulse shape.

All these methods [and other variants such as self-diffraction and polarization-gate FROG, the use of a frequency filter in one arm,[10,11] and spectral phase interferometry for direct electric-field reconstruction (SPIDER)[5]] have inherent ambiguities. For example, all such self-referenced techniques fail to determine the absolute phase and the arrival time—the first two coefficients in the Taylor series expansion of the spectral phase. These two ambiguities are actually usually desirable. The absolute phase is random in fluorescent pulses and prevents techniques such as spectral interferometry, that do measure absolute phase relative to that of another pulse, from measuring fluorescence on a multishot basis. Measurement of the pulses' arrival times are also generally not of interest because few researchers care about the distance between the laser and the pulse-measurement device or desire to stabilize this quantity interferometrically.

Other ambiguities are potentially more serious. For example, the most commonly used version of FROG, second-harmonic generation (SHG) FROG,[12] has a twofold ambiguity: A pulse and its time-reversed replica give the same trace.[13] This ambiguity can be resolved by addition of a trailing satellite pulse or by use of higher-order variants such as self-diffraction and polarization-gate FROG, or with SPIDER.[5] Determining the relative phase of two pulses with the same center frequency but a large time separation, which is important for coherent manipulations, also provides a challenge for some techniques, despite the fact that this information is contained directly in the linear spectrum. The relative phase is completely unknown in spectrograms generated by the cross-correlated version of FROG[14,15] (XFROG) when the gate pulse is short compared with the temporal separation. The self-referenced SHG FROG has a twofold ambiguity for such pulses: If the relative phase is φ, then the value $\varphi+\pi$ also yields the same SHG FROG trace. Third-harmonic-generation (THG) FROG has a threefold

ambiguity in the relative phase of well-separated temporal components: $\varphi = \pm 2\pi/3$ also yield the same THG FROG trace (thus a combination of methods can resolve this ambiguity). Other versions of FROG, however, uniquely determine this relative phase.

In this paper we treat the waveforms that contain significant gaps in their frequency profiles,[17] expanding on the preliminary results presented in Ref. 16. Such waveforms are simply made and have some straightforward applications (for example, coherent pumping of Raman transitions). Already, single-color phase-locked pulses have been used in various kinds of nonlinear spectroscopic studies, such as the detection of optical free-induction decay,[18] phase-locked pump–probe,[19] and heterodyne detected photon echo.[20] The next step might be to use phase-locked multicolor pulses. Such pulses may also be used for optimal control of chemical dynamics. For example, in a pump–dump experiment, theoretical studies[21] have indicated that, for control of population transfer between states of a chemical system, the relative phase of the two colored pump and dump pulses is important. To that effect, a recent Letter reported the generation of such pulses by use of noncollinear optical amplification of shaped white-light continua.[22] In optical communications, dense wavelength-division multiplexing with ultrafast pulses inherently involves generating precisely this type of waveform,[23,24] and complex time–frequency patterns with gaps are useful for suppression of multipath interference.[25] Unlike for same-frequency pulses, the relative phase of frequency-separated pulses does not show up in the linear spectrum, even if the pulses overlap in time.

It was previously noted[3] that the spectrogram is mathematically equivalent to the sonogram: Gating in the time domain yields an expression that is equivalent to that obtained by gating in the frequency domain, except for a reversed argument in the gate function. Thus it would seem reasonable that a similar ability to measure the relative phase (with the occasional ambiguities touched on above) is possible in the frequency domain for well-separated frequency components. We show here, however, that none of the published self-referenced methods determines the relative phase of well-separated frequency components. Furthermore, if these well-separated frequency components are also well separated in time, the cross-correlation variants (e.g., XFROG) that use independent pulses as gates fail as well, unless the gating or spectral interference occurs with short, well-characterized pulses (which might be characterized by a self-referenced method) whose spectral widths span the spectral distance between the components. This is equivalent to requiring that the gate or reference pulse be sufficiently short to resolve the temporal structure in the pulse that results from the well-separated frequency components of the pulse to be measured. This constraint is analogous to that on the gate pulse in XFROG for measuring pulses separated in time. We also derive specific conditions under which modified versions of the cross-referenced techniques do give full pulse characterization.

At a qualitative level, the existence of ambiguities in characterizing the time–frequency profiles of frequency-separated pulses is easy to understand. Without loss of generality, any arbitrary waveform can be written as a combination of amplitude and phase modulation:

$$E(\omega) = \tilde{A}(\omega)\exp[i\tilde{\varphi}(\omega)] + \text{c.c.}, \tag{1}$$

where $\tilde{A}(\omega)$ is a real nonnegative function and $\tilde{\varphi}(\omega)$ is the frequency-dependent phase. For most pulse-characterization methods, however, it is more intuitive to describe the pulse shape by amplitudes $A(\omega)$ of its frequency components and their arrival times $t(\omega)$, where $t(\omega) = \mathrm{d}\tilde{\varphi}(\omega)/\mathrm{d}\omega$. From this relationship, knowledge of $\varphi(\omega)$ in a small interval about ω is all that is required for extraction of $t(\omega)$. However, extracting $\varphi(\omega)$ from $t(\omega)$ requires an integral over all times before ω—including frequencies at which the waveform might actually vanish. Thus reproducing the actual waveform (in particular, the relative phase of two different parts of the pulse) can present inherent difficulties if the experimental information is present as a time–frequency profile, such as in a sonogram.

It is less obvious that such ambiguities persist for FROG and other methods that use the entire pulse as its own reference. To demonstrate the ambiguities that arise in the characterization of multifrequency phase-locked pulses (and in general any pulse containing well-separated frequency components), we use a two-component pulse that can be described by (see also Appendix A)

$$\begin{aligned} E(t) = {} & A_A(t)\exp(-i\omega_A t)\exp(i\phi_A) \\ & + A_B(t - T)\exp(-i\omega_B t)\exp(i\phi_B), \end{aligned} \tag{2}$$

$$\begin{aligned} E(\omega) = {} & |\tilde{A}_A(\omega - \omega_A)|\exp[i\tilde{\phi}_A(\omega - \omega_A)]\exp(i\phi_A) \\ & + |\tilde{A}_B(\omega - \omega_B)|\exp[i\tilde{\phi}_B(\omega - \omega_B)] \\ & \times \exp(i\phi_B), \end{aligned} \tag{3}$$

where $|\tilde{A}(\omega)|\exp[i\tilde{\varphi}(\omega)] = \int \mathrm{d}t A(t)\exp(i\omega t)$.

Thus, this pulse contains one component, centered about $\omega = \omega_A$, with spectral width $\delta\omega$ and arriving at $t = 0$ with pulse length δt, followed after time T by the second component, centered about $\omega = \omega_B$. The two components have a well-defined phase difference $\phi_A - \phi_B$. For later convenience, we split the phase in the frequency domain into two parts, $\tilde{\varphi}(\omega) = \tilde{\phi}(\omega) + \phi_X$, where the first term represents the phase within each component and ϕ_X represents the overall phase of component X.

The question that we investigate in this paper is under what circumstances current pulse-characterization techniques are capable of determining phase difference $\phi_A - \phi_B$ between the two components of the pulse. For most of the examples in this paper we use a pulse consisting of two Gaussian components:

$$\begin{aligned} E(t) = {} & \exp(-\alpha^2 t^2)\exp(-i\omega_A t)\exp(i\phi_A) \\ & + \exp[-\alpha^2(t - T)^2]\exp(-i\omega_B t)\exp(i\phi_B). \end{aligned} \tag{4}$$

However, the arguments made here can readily be extended to other shapes and to pulses consisting of multiple well-separated spectral components.

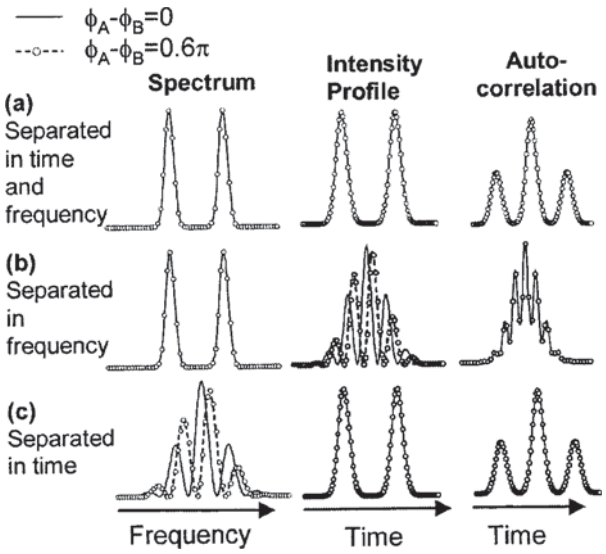

Fig. 1. Comparison of the spectrum, the intensity profile, and autocorrelation of pulses described by Eq. (4) for $\phi_A - \phi_B = 0$ (solid curves) and $\phi_A - \phi_B = 0.6\pi$ (dashed curves). (a) Components of a pulse are well separated in both the time and the frequency domains ($T \gg \delta t$ and $\Delta\omega \gg \delta\omega$). (b) Components overlap in the time domain but are well separated in the frequency domain ($T = 0$ and $\Delta\omega \gg \delta\omega$). (c) Components are well separated in the time domain but overlap in the frequency domain ($T \gg \delta t$ and $\Delta\omega = 0$). If the components do not overlap in the frequency domain [(a) and (b)], then the spectrum and the autocorrelation are identical for every $\phi_A - \phi_B$. Only if the components of the pulse overlap in the frequency domain [(c)] can the phase relation between the components be determined from the spectrum.

If the pulses are well separated in both the time and the frequency domains (i.e., $\Delta\omega = \omega_A - \omega_B \gg \delta\omega$ and $T \gg \delta t$), then the temporal intensity profile, the autocorrelation, and the spectrum are all identical for all phase differences $\phi_A - \phi_B$ between the components of the pulse [Fig. 1(a)]. For pulses separated in the frequency domain but with overlap in the time domain (i.e., $T < \delta t$), the phase difference $\phi = \phi_A - \phi_B$ is reflected in the temporal intensity profile; however, in the simplest pulse-characterization methods, the autocorrelation and the spectrum, this relative phase is not detectable [Fig. 1(b)]. Only for pulses that overlap in the frequency domain ($\omega_A - \omega_B < \delta\omega$) can the overall phase difference be readily detected in the spectrum [Fig. 1(c)]. Therefore in this paper we concentrate on the first two cases, i.e., pulses that are well separated in the frequency domain. In the next sections we discuss the performance of several characterization techniques (FROG and SPIDER and their derivatives) on the types of pulse described above.

2. SECOND-HARMONIC GENERATION FROG

The spectrogram obtained in SHG FROG is given by[3]

$$I^{\mathrm{SHG}}(\Omega, \tau) = \left| \int E(t)E(t-\tau)\exp(i\Omega t)\mathrm{d}t \right|^2. \quad (5)$$

Using Eq. (2) for $E(t)$ yields for the FROG trace for this pulse

$$\begin{aligned} I^{\mathrm{SHG}}(\Omega, \tau) = \Big| & \exp(i\omega_A\tau)\exp(2i\phi_A) \\ & \times \int A_A(t)A_A(t-\tau)\exp[i(\Omega - 2\omega_A)t]\mathrm{d}t \\ & + \exp(i\omega_B\tau)\exp[i(\phi_A + \phi_B)] \\ & \times \int A_A(t)A_B(t-T-\tau) \\ & \times \exp[i(\Omega - \omega_A - \omega_B)t]\mathrm{d}t \\ & + \exp(i\omega_A\tau)\exp[i(\phi_A + \phi_B)] \\ & \times \int A_B(t-T)A_A(t-\tau) \\ & \times \exp[i(\Omega - \omega_A - \omega_B)t]\mathrm{d}t \\ & + \exp(i\omega_B\tau)\exp(2i\phi_B) \\ & \times \int A_B(t-T)A_B(t-T-\tau) \\ & \times \exp[i(\Omega - 2\omega_B)t]\mathrm{d}t \Big|^2. \end{aligned} \quad (6)$$

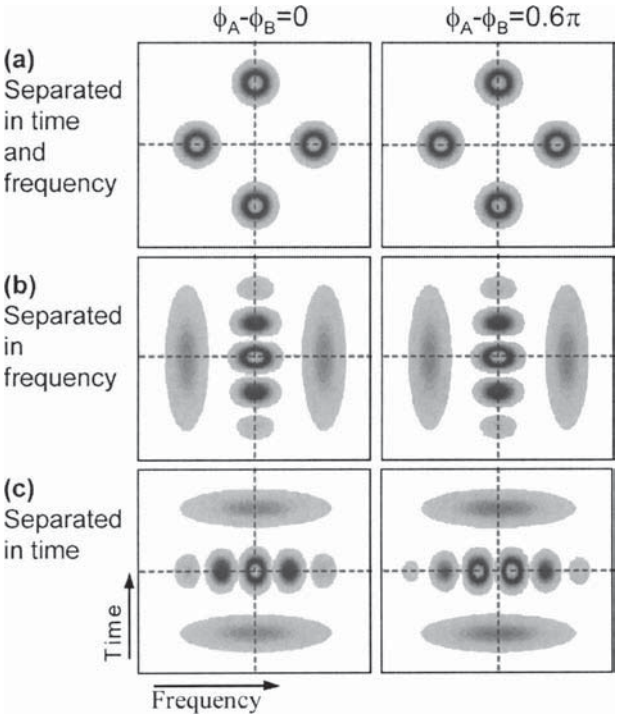

Fig. 2. Comparison of SHG FROG spectrograms for pulses described by Eq. (4) with $\phi_A - \phi_B = 0$ (left) and $\phi_A - \phi_B = 0.6\pi$ (right). (a) SHG FROG spectrogram for a pulse with components well separated in the time domain and in the frequency domain. (b) Spectrogram for a pulse with components well separated in the frequency domain but overlapping in the time domain. (c) Spectrogram for a pulse with components well separated in the time domain but overlapping in the frequency domain. The spectrograms for pulses that are well separated in the frequency domain [(a) and (b)] are identical for all phase differences $\phi_A - \phi_B$. Only if the pulses overlap in the frequency domain [(c)] can the SHG FROG determine phase difference $\phi_A - \phi_B$.

In Eq. (6) the first term results in a peak centered about $\Omega = 2\omega_A$ and $\tau = 0$; the second term gives a peak centered about $\Omega = \omega_A + \omega_B$ and $\tau = -T$; the third term results in a peak about $\Omega = \omega_A + \omega_B$ and $\tau = T$, and the fourth term gives a peak centered about $\Omega = 2\omega_B$ and $\tau = 0$ [Fig. 2(a)]. For the most commonly encountered case in which $\omega_A = \omega_B$, the beating between the first and the fourth terms creates fringes proportional to $1 + \cos[(\Omega - 2\omega_A)T + 2(\phi_B - \phi_A)]$ and, subject to the π-phase ambiguity, the phase relation can be readily recovered [Fig. 2(c)]. If, however, the components of the pulse are well separated in the frequency domain, then there are no cross terms among these three groups of terms, so interference occurs only between the second and third terms in Eq. (6), and then only if the two components overlap in the time domain (i.e., $T \ll \delta t$). But, as can be seen, both terms have the same dependence on phases ϕ_A and ϕ_B. In this case the position of the interference fringes is proportional to $1 + \cos[(\omega_A - \omega_B)\tau]$ and depends only on frequency difference $\omega_A - \omega_B$, not on relative phase $\phi_A - \phi_B$ [Fig. 2(b)], so the retrieval algorithm cannot distinguish among different values of the phase difference.

The fact that FROG can readily determine the phase difference between two components of a pulse that are separated in the time domain, but not between two components separated in the frequency domain, may be surprising because the SHG FROG spectrogram can be rewritten in the frequency domain as

$$I^{\mathrm{SHG}}(\Omega, \tau) = \left| \int E(\omega) E(\Omega - \omega) \exp(i\omega\tau) \mathrm{d}\omega \right|^2, \quad (7)$$

which is similar to the expression given in Eq. (5). The main difference between pulses with components separated in the frequency domain and those with components separated in the time domain lies in which terms contribute to the same peak in the spectrogram. For components separated in the time domain, terms generated from component A interacting with its delayed copy A, and component B interacting with the delayed copy of component B, contribute to the central term at $\tau = 0$. As these two terms have different dependence on ϕ_A and ϕ_B, an interference pattern results that depends on the phase difference $\phi = \phi_A - \phi_B$. If the components are separated in the frequency domain, it is the contributions that result from the cross terms, i.e., component A interacting with B and vice versa, that contribute to the central peak at $\omega = \omega_A + \omega_B$, and as a result all terms that contribute to this central peak have the same dependence on phases ϕ_A and ϕ_B, and the spectrogram is independent of $\phi_A - \phi_B$.

3. POLARIZATION-GATE FROG

The spectrogram for polarization-gate (PG) FROG can be described as[3]

$$I^{\mathrm{PG}}(\Omega, \tau) = \left| \int E(t) |E(t - \tau)|^2 \exp(i\Omega t) \mathrm{d}t \right|. \quad (8)$$

For the pulse described by Eq. (2) the spectrogram becomes

$$\begin{aligned} I^{\mathrm{PG}}(\Omega, \tau) = \Bigg| & \exp(i\phi_A) \int A_A(t) |A_A(t - \tau)|^2 \exp[i(\Omega - \omega_A)t] \mathrm{d}t \\ & + \exp(i\phi_A) \int A_A(t) |A_B(t - T - \tau)|^2 \exp[i(\Omega - \omega_A)t] \mathrm{d}t \\ & + \exp[i(\omega_A - \omega_B)\tau] \exp(i\phi_A) \int A_B(t - T) A_A(t - \tau) A_B^*(t - T - \tau) \exp[i(\Omega - \omega_A)t] \mathrm{d}t \\ & + \exp(i\phi_B) \int A_B(t - T) |A_B(t - T - \tau)|^2 \exp[i(\Omega - \omega_B)t] \mathrm{d}t \\ & + \exp(i\phi_B) \int A_B(t - T) |A_A(t - \tau)|^2 \exp[i(\Omega - \omega_B)t] \mathrm{d}t \\ & + \exp[i(\omega_B - \omega_A)\tau] \exp(i\phi_B) \int A_A(t) A_B(t - T - \tau) A_A^*(t - \tau) \exp[i(\Omega - \omega_B)t] \mathrm{d}t \\ & + \exp[i(\omega_A - \omega_B)\tau] \exp[i(2\phi_A - \phi_B)] \int A_A(t) A_A(t - \tau) A_B^*(t - T - \tau) \exp[i\{\Omega - (2\omega_A - \omega_B)\}t] \mathrm{d}t \\ & + \exp[i(\omega_B - \omega_A)\tau] \exp[i(2\phi_B - \phi_A)] \int A_B(t - T) A_B(t - T - \tau) \\ & \times A_A^*(t - \tau) \exp\{i[\Omega - (2\omega_B - \omega_A]t\} \mathrm{d}t \Bigg|^2. \quad (9) \end{aligned}$$

As can be seen from Eq. (9) the first three terms result in a peak centered about ω_A, the second three terms give a peak centered about ω_B, the seventh term gives a peak about $2\omega_A - \omega_B$, and finally the eighth term yields a peak about $2\omega_B - \omega_A$. If the frequencies ω_A and ω_B of the two components are well separated, the cross terms

between these groups will vanish. As for the SHG spectrogram, the terms that contribute to a peak at the same spectral position in the spectrogram have the same dependence on phases ϕ_A and ϕ_B, so if the peaks are well separated the intensity of the spectrogram will not depend on the relative phase $\phi_A - \phi_B$ [Figs. 3(a) and 3(b)]. Only if the components of the pulse overlap in the frequency domain can the relative phase be determined [Figs. 3(c) and 3(d)]. The same is true for all other forms of self-referenced FROG because, in all these techniques, all terms that contribute at a certain spectral position must have been generated from the same set of components of the pulse and thus must have the same dependence on ϕ_A and ϕ_B. In other words, a term that contributes to the spectrogram at position $x\omega_A + y\omega_B$ will always have the phase dependence $x\phi_A + y\phi_B$. Thus, for all types of self-referenced FROG, so long as there is no overlap between the individual peaks in the spectrogram[26] this spectrogram will be independent of the phase relation between the spectral components of the pulse.

4. SPIDER

The SPIDER technique fares no better. The interferogram obtained by SPIDER[5] is given by

$$
\begin{aligned}
&I^{\mathrm{SPIDER}}(\omega) \\
&\quad = |E(\omega-\omega_0)E(\omega_0) + E(\omega-\omega_0-\Omega)E(\omega_0+\Omega) \\
&\qquad \times \exp(-i\phi_S)\exp(i\omega\tau)|^2 \\
&\quad = |E(\omega-\omega_0)E(\omega_0)|^2 \\
&\qquad + |E(\omega-\omega_0-\Omega)E(\omega_0+\Omega)|^2 \\
&\qquad + 2\,\mathrm{Re}[E(\omega-\omega_0)E^*(\omega-\omega_0-\Omega)E(\omega_0) \\
&\qquad \times E^*(\omega_0+\Omega)\exp(i\phi_S)\exp(-i\omega\tau)]. \qquad (10)
\end{aligned}
$$

In Eq. (10) it has been assumed that the stretched pulse is stretched far enough that it is essentially monochromatic over the duration of the probe pulse. ω is the frequency of the upconverted signal; ω_0 is this monochromatic frequency of the stretched pulse at the time that it overlaps the first copy of the test pulse. $\Omega = \tau/2\beta$ is the spectral shear, which is related to delay τ between the two copies of the test pulse and to chirp parameter β of the stretched pulse. Then $\omega_0 + \Omega$ is the monochromatic frequency of the stretched pulse at the time that the second copy of the probe pulse arrives. $\phi_S = \omega_0\tau + \tau^2/4\beta$ is a constant phase.

So long as $I(\omega)$ is independent of $\phi_A - \phi_B$ (i.e., when the components are well separated in the frequency domain), the first two terms in Eq. (10) are independent of the phases ϕ_A and ϕ_B. Using Eq. (3) in the third term of Eq. (10) gives

$$
\begin{aligned}
&2\,\mathrm{Re}(\{\tilde{A}_A(\omega-\omega_A-\omega_0)\exp[i\tilde{\phi}_A(\omega-\omega_A-\omega_0)]\exp(i\phi_A) + \tilde{A}_B(\omega-\omega_B-\omega_0)\exp[i\tilde{\phi}_B(\omega-\omega_B-\omega_0)]\exp(i\phi_B)\} \\
&\quad \times \{\tilde{A}_A(\omega-\omega_A-\omega_0-\Omega)\exp[-i\tilde{\phi}_A(\omega-\omega_A-\omega_0-\Omega)]\exp(-i\phi_A) \\
&\quad + \tilde{A}_B(\omega-\omega_B-\omega_0-\Omega)\exp[-i\tilde{\phi}_B(\omega-\omega_B-\omega_0-\Omega)]\exp(-i\phi_B)\} \\
&\quad \times \{\tilde{A}_A(\omega_0-\omega_A)\exp[i\tilde{\phi}_A(\omega_0-\omega_A)]\exp(i\phi_A) + \tilde{A}_B(\omega_0-\omega_B)\exp[i\tilde{\phi}_B(\omega_0-\omega_B)]\exp(i\phi_B)\} \\
&\quad \times \{\tilde{A}_A(\omega_0+\Omega-\omega_A)\exp[-i\tilde{\phi}_A(\omega_0+\Omega-\omega_A)]\exp(-i\phi_A) + \tilde{A}_B(\omega_0+\Omega-\omega_B) \\
&\quad \times \exp[-i\tilde{\phi}_B(\omega_0+\Omega-\omega_B)\exp(-i\phi_B)\}\exp(i\phi_S)\exp(-i\omega\tau)). \qquad (11)
\end{aligned}
$$

It can be seen that there will be a signal only if ω_0 is close to either ω_A or ω_B. Without loss of generality, in this example we choose ω_0 close to ω_A, i.e., $\omega_0 - \omega_A < \delta\omega$. To fulfill the requirement that Ω be smaller than the Nyquist limit, $\omega_0 + \Omega$ also has to be close to ω_A; i.e., $\omega_0 + \Omega - \omega_A < \delta\omega$. Then both copies of the test pulse are upconverted by a quasi-cw part of component A of the stretched pulse, and Eq. (11) becomes

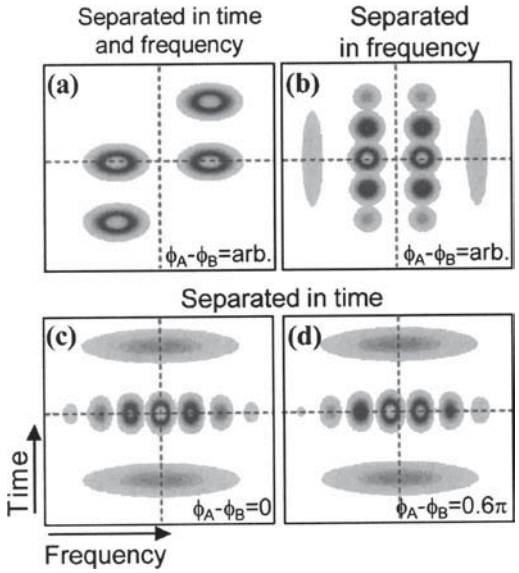

Fig. 3. Comparison of PG FROG spectrograms for pulses described by Eq. (4). (a) PG FROG spectrogram for a pulse with components separated both in the time domain and in the frequency domain. (b) Spectrogram for a pulse with components well separated in the frequency domain but arriving at the same time. (c) Spectrogram for a pulse with components at the same frequency but well separated in the time domain, with $\phi_A - \phi_B = 0$. (d) Same as (c) but with $\phi_A - \phi_B = 0.6\pi$. The spectrograms for pulses well separated in the frequency domain [(a) and (b)] are identical for all phase differences $\phi_A - \phi_B$. Only if the pulses overlap in the frequency domain can the PG FROG determine the phase difference $\phi_A - \phi_B$.

$$
\begin{aligned}
2\,\mathrm{Re}(\{&\tilde{A}_A(\omega-\omega_A-\omega_0)\exp[i\tilde{\phi}_A(\omega-\omega_A-\omega_0)]\exp(i\phi_A)\tilde{A}_A(\omega-\omega_A-\omega_0-\Omega)\exp[-i\tilde{\phi}_A(\omega-\omega_A-\omega_0-\Omega)]\\
&\times\exp(-i\phi_A)+\tilde{A}_A(\omega-\omega_A-\omega_0)\exp[i\tilde{\phi}_A(\omega-\omega_A-\omega_0)]\exp(i\phi_A)\tilde{A}_B(\omega-\omega_B-\omega_0-\Omega)\\
&\times\exp[-i\tilde{\phi}_B(\omega-\omega_B-\omega_0-\Omega)]\exp(-i\phi_B)+\tilde{A}_B(\omega-\omega_B-\omega_0)\exp[i\tilde{\phi}_B(\omega-\omega_B-\omega_0)]\\
&\times\exp(i\phi_B)\tilde{A}_A(\omega-\omega_A-\omega_0-\Omega)\exp[-i\tilde{\phi}_A(\omega-\omega_A-\omega_0-\Omega)]\exp(-i\phi_A)+\tilde{A}_B(\omega-\omega_B-\omega_0)\\
&\times\exp[i\tilde{\phi}_B(\omega-\omega_B-\omega_0)]\exp(i\phi_B)+\tilde{A}_B(\omega-\omega_B-\omega_0-\Omega)\exp[-i\tilde{\phi}_B(\omega-\omega_B-\omega_0-\Omega)]\exp(-i\phi_B)\}\\
&\times\tilde{A}_A(\omega_0-\omega_A)\exp[i\tilde{\phi}_A(\omega_0-\omega_A)]\exp(i\phi_A)\tilde{A}_A(\omega_0+\Omega-\omega_A)\exp[-i\tilde{\phi}_A(\omega_0+\Omega-\omega_A)]\\
&\times\exp(-i\phi_A)\exp(i\phi_S)\exp(-i\omega\tau)).
\end{aligned}
\tag{12}
$$

The only nonzero contributions to Eq. (12) are given by the first and fourth terms, which result in a signal centered about $\omega = 2\omega_A$ and $\omega = \omega_A + \omega_B$, respectively. As can be seen from Eq. (12), both terms are independent of ϕ_A and ϕ_B. The reason for this is that the two peaks in the SPIDER spectrum are the SPIDER spectra of the individual components of the pulse, but there is no part in the spectrum that is generated by interference of the two components. Thus in this case the relative phase within each pulse, $\tilde{\phi}$, can be determined accurately, but the overall phase difference between the two components remains undetermined.

For larger spectral shear, i.e., when $\omega_0 - \omega_A + \Omega \gg \delta\omega$, in general there is no nonzero contribution to Eq. (11) except when Ω is chosen such that the original test pulse is upconverted by a quasi-cw part of component A of the stretched pulse and the delayed copy is upconverted by a part of component B of the stretched pulse, i.e., $\omega_0 \approx \omega_A$ and $\omega_0 + \Omega \approx \omega_B$. In that case, interference occurs near frequency $\omega = \omega_A + \omega_B$ between component B of the original pulse upconverted by a quasi-cw part of component A of the stretched pulse and component A of the delayed copy upconverted by a quasi-cw part of component B of the stretched pulse. However, just as for FROG, the two interfering terms have the same dependence on ϕ_A and ϕ_B, and this final interferogram is still independent of $\phi_A - \phi_B$ (see also the discussion in Section 6 below).

From the discussion above it can be concluded that none of the self-referencing techniques discussed is able to detect the phase difference between two spectrally separated parts of a laser pulse. However, spectral interferometry[27] is capable of retrieving the complete phase of such a pulse, as long as a reference pulse is available that spectrally overlaps all the spectral components of the pulse that needs to be characterized and is well characterized, i.e., as long as complete phase and amplitude information is available for this reference pulse.

Such a reference pulse is not always available; therefore in Sections 5 and 6 we consider whether XFROG[14,15] and the cross-correlation version of SPIDER[28,29] (XSPIDER) would impose less stringent requirements on the reference pulse used.

5. XFROG

As an example of an XFROG technique, we discuss sum-frequency generation (SFG) XFROG, but, as before, the results apply to all the XFROG beam geometries. The SFG XFROG interferogram can be written as[14]

$$
I^{\mathrm{XSFG}}(\Omega,\tau) = \left|\int E(t)E_X(t-\tau)\exp(i\Omega t)\mathrm{d}t\right|^2, \tag{13}
$$

where $E(t)$ is the electric field of the pulse to be characterized, i.e., the test pulse, and $E_X(t)$ is the electric field of the reference pulse. It is assumed that both the phase and the amplitude of this reference pulse are known. Equation (6) now becomes

$$
\begin{aligned}
I^{\mathrm{XSFG}}(\Omega,\tau) = \Bigg|&\exp(i\omega_0\tau)\exp(i\phi_A)\int A_A(t)A_X(t-\tau)\\
&\times\exp[i(\Omega-\omega_A-\omega_0)t]\mathrm{d}t\\
&+\exp(i\omega_0\tau)\exp(i\phi_B)\int A_B(t-T)\\
&\times A_X(t-\tau)\exp[i(\Omega-\omega_B-\omega_0)t]\mathrm{d}t\Bigg|^2,
\end{aligned}
\tag{14}
$$

where ω_0 is now the center frequency of the reference. This spectrogram will depend on the relative phase $\phi_A - \phi_B$ only if the cross terms in Eq. (14) are nonzero, which means only if the two terms overlap both in the frequency domain and in the time domain. If the two components overlap in the time domain but not in the frequency domain, the reference pulse must be broadband—i.e., very short—with a maximum pulse length $\delta t_X \approx 2\pi/\Delta\omega$. This is equivalent to the condition that the reference pulse be able to resolve the temporally sinusoidal intensity variations that are due to the two frequencies. Thus, if the components of the pulse overlap in the time domain, such a short reference pulse will make it possible to determine $\phi_A - \phi_B$ [Figs. 4(a) and 4(b)].

If the frequency components in the pulse do not overlap in time [$T \gg \delta t$ in Eq. (2)], then a short reference pulse will fail to connect the frequency components in delay, and no interference will be observed [Fig. 4(c)]. What is needed is a pulse that is "doubly broad," that is, broad in both frequency and time. Two examples of such doubly broad pulses are a pulse train of short reference pulses and a linearly chirped pulse. In both cases, however,

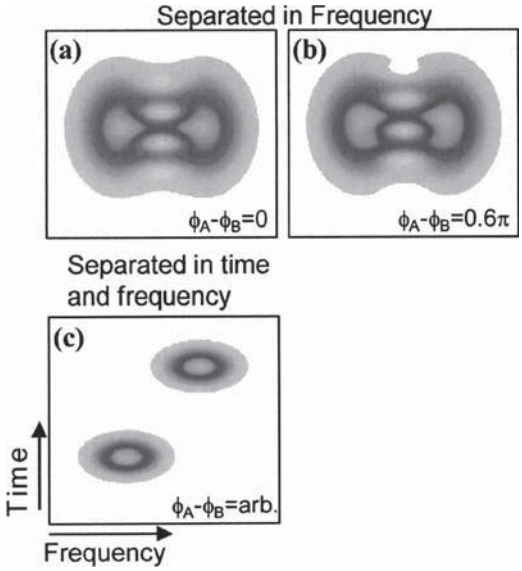

Fig. 4. Comparison of SFG XFROG spectrogram for pulses described by Eq. (4). (a) SFG XFROG spectrogram for pulse with components well separated in the frequency domain but overlapping in time, with $\phi_A - \phi_B = 0$. (b) Same as (a) but with $\phi_A - \phi_B = 0.6\pi$. Here a reference pulse is used that is just short enough to cause the two peaks in the spectrogram to overlap such that interference fringes can be observed. The position of the fringes permits determination of $\phi_A - \phi_B$. If a longer reference is used, the two peaks in the spectrogram do not overlap, and $\phi_A - \phi_B$ cannot be determined. (c) The same reference as for (a) and (b) was used but the components of the pulse were well separated both in the time domain and in the frequency domain. Now the spectrogram is identical for all phase differences $\phi_A - \phi_B$.

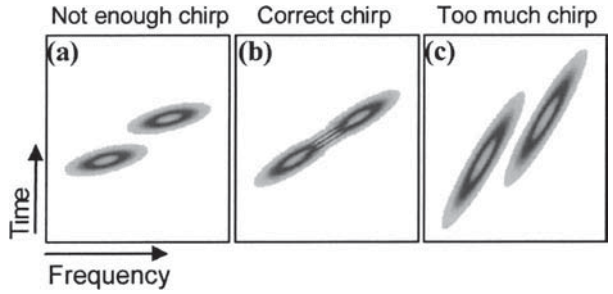

Fig. 5. SFG XFROG diagram for the pulses depicted in Fig. 4(c) (separated both in frequency and in time), with a chirped reference pulse. If the amount of chirp imposed on the reference is (a) not enough or (c) too much, no interference is observed, and the phase difference between the components cannot be determined. Only if the pulse is chirped by the correct amount (b) can an interference pattern be observed that permits determination of $\phi_A - \phi_B$.

prior knowledge about the arrival time and frequencies of the components is needed. For a linearly chirped pulse the amount of chirp needs to be matched to the delay and to the frequency difference between the components of the test pulse. For example, if at a delay τ component A overlaps a part of the reference pulse centered about $\omega_{A\mathrm{ref}}$, then the corresponding peak in the spectrogram will be centered about $\omega_A + \omega_{A\mathrm{ref}}$. Component B will then overlap frequency $\omega_{B\mathrm{ref}} = \omega_{A\mathrm{ref}} + \Omega_{\mathrm{chirp}}$, where Ω_{chirp} is determined by the amount of linear chirp imposed on the reference pulse and on the delay between components A and B. Thus the peak in the spectrogram that corresponds to component B will be centered about $\omega_B + \omega_{A\mathrm{ref}} + \Omega_{\mathrm{chirp}}$. Information about phase difference $\phi_A - \phi_B$ will be available only if these two peaks overlap in the frequency domain, i.e., if $\Omega_{\mathrm{chirp}} = \omega_A - \omega_B$. In other words, the amount of chirp needs to be chosen carefully to ensure that the reference pulse connects the components in both the time and the frequency domains. If the chirp is chosen correctly the two peaks will overlap in the spectrogram, and the resultant interference will reveal the phase difference, $\phi_A - \phi_B$ [Fig. 5(b)]. If the amount of chirp is too large or too small, then there will be no overlap between the two peaks in the spectrogram, and no information about $\phi_A - \phi_B$ will be obtained [Figs. 5(a) and 5(c)].

In general, for a pulse with more than two components whose spacings in time and frequency are uncorrelated, it will be impossible to find a linearly chirped pulse that will connect all the components. In that case, to obtain full characterization, one would need to repeat the experiment with a different chirp matched to each pair of components in the pulse.

An alternative way to create a doubly broad pulse is to use an etalon. The etalon increases the temporal width of the pulse by introducing delayed replicas of the original pulse into the beam while preserving the overall spectral width of the original pulse. Care must be taken in the selection of the etalon. If the etalon spacing is too great, there will be dead spaces between the individual pulses of the reference. These dead spaces would allow the individual terms of Eq. (13) to occupy the same regions but with zero signal overlap.

To summarize, if all spectral components of the pulse arrive at a similar time, an XFROG measurement with a well-characterized short pulse can determine the overall phase relation among the components. In all other cases it is, in principle, possible to determine the phase difference among the components by using a correctly chirped reference pulse or pulse train. The requirements on the reference pulse are then less stringent than in the case of spectral interference because the reference pulse need not have the same center frequency as the test pulse. But, in addition to the requirement of large bandwidth, there are now requirements on the pulse length: A transform-limited short pulse is needed if the pulse components arrive at the same time and a properly chirped pulse or pulse train is needed if they arrive at different times.

6. XSPIDER

One obtains an XSPIDER[28,29] spectrogram by sending the test pulse through a Michelson interferometer to generate a train of two test pulses, gating this train with a chirped reference pulse, and then spectrally resolving the gated pulse.

Assuming that a well-known reference pulse is available to provide the stretched pulse, the expression for the XSPIDER spectrum becomes[29]

$$I^{\mathrm{XSPIDER}}(\omega) = |E(\omega-\omega_0)E_X(\omega_0)|^2 + |E(\omega-\omega_0-\Omega)E_X(\omega_0+\Omega)|^2 + 2\,\mathrm{Re}[E(\omega-\omega_0)E^*(\omega-\omega_0-\Omega)E_X(\omega_0)E_X^*(\omega_0+\Omega)\exp(i\phi_S)\exp(-i\omega\tau)]. \quad (15)$$

For a small spectral shear Ω, following the same reasoning that leads to Eq. (12) yields the nonzero contributions to the phase-dependent part of I^{XSPIDER}:

$$\begin{aligned}2\,\mathrm{Re}\{&\tilde{A}_A(\omega-\omega_A-\omega_0)\exp[i\tilde{\phi}_A(\omega-\omega_A-\omega_0)]\exp(i\phi_A)\tilde{A}_A(\omega-\omega_A-\omega_0-\Omega)\\ &\times\exp[-i\tilde{\phi}_A(\omega-\omega_A-{}_0-\Omega)]\exp(-i\phi_A)+\tilde{A}_B(\omega-\omega_B-\omega_0)\exp[i\tilde{\phi}_B(\omega-\omega_B-\omega_0)]\\ &\times\exp(i\phi_B)\tilde{A}_B(\omega-\omega_B-\omega_0-\Omega)\exp[-i\tilde{\phi}_B(\omega-\omega_B-\omega_0-\Omega)]\exp(-i\phi_B)\}\\ &\times\tilde{A}_X(\omega_0)\exp[i\tilde{\varphi}_X(\omega_0)]\tilde{A}_X(\omega_0+\Omega)\exp[-i\tilde{\varphi}_X(\omega_0+\Omega)]\exp(i\phi_S)\exp(-i\omega\tau)).\end{aligned} \quad (16)$$

Both terms are independent of ϕ_A and ϕ_B, and again each peak represents the XSPIDER spectrum of the individual components of the test pulse [Fig. 6(a)].

In general, for larger spectral shear there is no nonzero contribution to the phase-dependent part of Eq. (14). However, just as in the case of an XFROG with a linearly chirped reference, a nonzero component exists if the spectral shear is chosen such that upconverted component A of the original pulse overlaps in the frequency domain with upconverted component B of the delayed pulse, or vice versa, in the frequency domain [i.e., $\Omega \pm (\omega_A-\omega_B) < \delta\omega$]. If $\Omega-(\omega_A-\omega_B) < \delta\omega$ is chosen, there will be a part of the SPIDER spectrum centered about $\omega_A+\omega_0$ at which interference occurs between the two components of the pulse. In this case the only nonzero contribution to the phase-dependent part of the XSPIDER spectrum is given by the XSPIDER equivalent of the first term of Eq. (12):

$$\begin{aligned}2\,\mathrm{Re}\{&\tilde{A}_A(\omega-\omega_A-\omega_0)\exp[i\tilde{\phi}_A(\omega-\omega_A-\omega_0)]\exp(i\phi_A)\tilde{A}_B(\omega-\omega_B-\omega_0-\Omega)\\ &\times\exp[-i\tilde{\phi}_B(\omega-\omega_B-\omega_0-\Omega)]\exp(-i\phi_B)\tilde{A}_X(\omega_0)\exp[i\tilde{\varphi}_X(\omega_0)]\tilde{A}_X(\omega_0+\Omega)\\ &\times\exp[-i\tilde{\varphi}_X(\omega_0+\Omega)]\exp(-i\phi_S)\exp(-i\omega\tau)\\ =|&\tilde{A}_A(\omega-\omega_A-\omega_0)\tilde{A}_B(\omega-\omega_B-\omega_0-\Omega)\tilde{A}_X(\omega_0)\tilde{A}_X(\omega_0+\Omega)|\\ &\times\cos[\tilde{\phi}_A(\omega-\omega_A-\omega_0)-\tilde{\phi}_B(\omega-\omega_B-\omega_0-\Omega)+\phi_A\\ &-\phi_B+\tilde{\varphi}_X(\omega_0)-\tilde{\varphi}_X(\omega_0+\Omega)+\phi_S-\omega\tau].\end{aligned} \quad (17)$$

Thus, so long as $\tilde{\phi}_A$, $\tilde{\phi}_B$, $\tilde{\varphi}_X$, ϕ_S, and $\omega\tau$ are known, $\phi_A-\phi_B$ can be determined [Fig. 6(b)]. However, for such a large spectral shear, which is much larger than the Nyquist limit, only information about the difference $\tilde{\phi}_A-\tilde{\phi}_B$ is obtained, and it is impossible to retrieve the full function $\tilde{\phi}(\omega)$ within each component. Thus, to obtain all the information, one requires a series of experiments. An XSPIDER with small spectral shear is required for $\tilde{\phi}_A(\omega)$ and $\tilde{\phi}_B(\omega)$. From this, the value of the large spectral shear, the value of Ω that is needed can be determined. Then a second XSPIDER experiment with this large spectral shear gives $\phi_A-\phi_B$. Note that, to obtain the absolute value of $\phi_A-\phi_B$, one needs ϕ_S, which requires knowledge of τ, ω_0, and Ω, all of which can be determined by calibration.[5] Thus in principle a combination of two experiments (together with the calibration experiments) could give the complete phase information, so long as the bandwidth of the reference is wide enough to give the proper spectral shear.

Again, if the pulse consists of more than two components that are not equally spaced, it is in general impossible to find a spectral shear Ω that will result in interference among all components. Then it becomes necessary to repeat the experiment with a different spectral shear Ω for each pair of components in the pulse and to obtain the phase information in a pairwise manner.

For XSPIDER the requirements on the reference pulse are the least stringent of the three methods discussed above. Just as in the case of SHG XFROG, the spectrum of the reference pulse does not need to overlap the test pulse as long as it is wide enough that it contains spectral components separated by $\Delta\omega=\omega_A-\omega_B$; however, un-

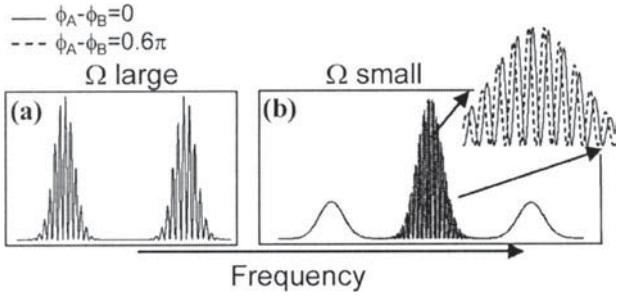

Fig. 6. XSPIDER spectrum for small spectral shear (left) and for large spectral shear (right), for pulses with $\phi_A-\phi_B=0$ and $\phi_A-\phi_B=0.6\pi$. The components are well separated both in time and in frequency. For small spectral shear, the two peaks in the SPIDER spectrum correspond to the SPIDER spectra of the individual components, and the spectrum is identical for all $\phi_A-\phi_B$. If the large spectral shear is chosen exactly correctly, the central peak in the spectrogram gives information about $\phi_A-\phi_B$ (inset), although now information about the phase within each component is not available.

like for SHG XFROG, there are no requirements on the length of the reference pulse as long as the pulse's phase is known.

7. SPECTRAL PHASE CONJUGATION SUM-FREQUENCY GENERATION FROG

As outlined above, a well-characterized reference is needed both for XFROG and for XSPIDER. In some cases, one needs a separate experiment to determine the arrival time of each of the components of the laser pulse, followed by one or more cross-correlated experiments to obtain the complete phase information. Therefore it would be advantageous to devise a self-referencing technique in which the information can be recovered with only one experiment.

In theory, if it is possible to create a spectral phase conjugate of the test pulse, one possible approach is to cross reference the test pulse with the spectral phase conjugation (SPC) of itself in a sum-frequency FROG. The spectrogram of such an experiment is

$$I^{\mathrm{SF-SPC}}(\Omega,\ \tau) = \left| \int E(t)E_{\mathrm{SPC}}(t\ -\ \tau)\exp(i\Omega t)\mathrm{d}t \right|^2. \quad (18)$$

The SPC copy E_{SPC} is related to original field E by

$$E_{\mathrm{SPC}}(\omega) = E^*(\omega), \quad (19)$$

and thus

$$E_{\mathrm{SPC}}(t) = A_{\mathrm{SPC}}(t)\exp(-i\omega t) = A^*(-t)\exp(-i\omega t). \quad (20)$$

If $E(t)$ is defined as in Eq. (2), then

$$E_{\mathrm{SPC}}(t) = A_A{}^*(-t)\exp(-i\omega_A t)\exp(-i\phi_A) + A_B{}^*(-t\ -\ T)\exp(-i\omega_B t)\exp(-i\phi_B). \quad (21)$$

The equivalent of Eq. (5) now becomes

$$I^{\mathrm{SF-SPC}}(\Omega,\ \tau) = \Bigg| \exp(i\omega_A\tau)\int A_A(t)A_A{}^*(-t\ -\ \tau)\exp[i(\Omega\ -\ 2\omega_A)t]\mathrm{d}t + \exp(i\omega_B\tau)\exp[i(\phi_A\ -\ \phi_B)]\int A_A(t)A_B{}^*(-t\ -\ T\ -\ \tau)\exp[i(\Omega\ -\ \omega_A\ -\ \omega_B)t]\mathrm{d}t + \exp(i\omega_A\tau)\exp\Big[i(-\phi_A\ +\ \phi_B]\int A_B(t\ -\ T)A_A{}^*(-t\ -\ \tau)\exp[i(\Omega\ -\ \omega_A\ -\ \omega_B)t]\mathrm{d}t + \exp(i\omega_B\tau)\int A_B(t\ -\ T)A_B{}^*(-t\ -\ T\ -\ \tau)\exp[i(\Omega\ -\ 2\omega_B)t]\mathrm{d}t \Bigg|^2. \quad (22)$$

The first and fourth terms in Eq. (22) result in peaks centered at $\tau = 0$, $\Omega = 2\omega_A$ and $\tau = -2T$, $\Omega = 2\omega_B$, respectively. The second and third terms both result in a peak centered at $\tau = -T$, $\Omega = \omega_A + \omega_B$ such that interference occurs between them, and the interference fringes can be described by $1 + \cos\{(\omega_A - \omega_B)\tau + [\Omega - (\omega_A + \omega_B)]T - 2(\phi_A - \phi_B)\}$.

Thus the phase relation among the components of the pulse can be retrieved in this experiment. The reason for this is that a spectral phase conjugated pulse can also be viewed as the time-reversed copy of the original pulse, where $t = 0$ is the reversal axis. In this case the pulse at delay T with phase ϕ_B will appear in the SPC copy as a pulse at delay $-T$ with phase $-\phi_B$. Hence, for a spectrogram peak at delay $\tau \sim T$, component A_A is upconverted with SPC component $A_B{}^*$ and has phase $\phi_A - \phi_B$, and A_B is upconverted with $A_A{}^*$ and thus has phase $\phi_B - \phi_A$. Both resultant peaks are at $\omega_A + \omega_B$. The beating between the two components provides the phase information. This is in contrast to the situation with the usual SHG FROG for which, if the components are also well separated in time, at $\tau \sim 0$ the only two components that contribute to the spectrogram are centered at different frequencies, $2\omega_A$ and $2\omega_B$, and do not beat against each other, so no phase difference can be recovered.

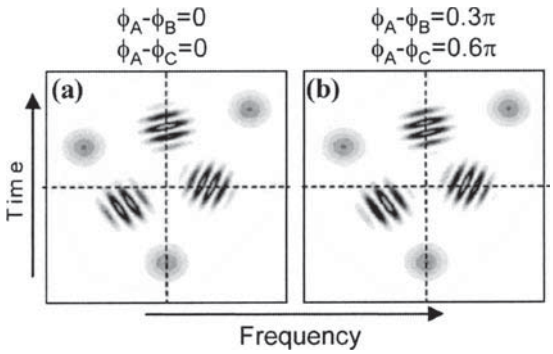

Fig. 7. Spectrogram of SPC SFG FROG for a pulse consisting of three components, all arriving at different times and with different center frequencies. In the spectrogram at the left, the phase difference among all components is zero; in the spectrogram at the right the phase difference between the first and the second components is 0.3π and between the first and third components is 0.6π. From the shift in the fringes, these phase differences can be recovered.

In general, for N different-colored pulses there will be $N(N-1)/2$ beating peaks on the spectrogram. Figure 7 shows, for example, a three-component case in which each component is well separated from the other two, both in the time domain and in the frequency domain. Any two of the beating peaks will provide enough information to enable the relative phases among the three pulses to be determined. Note that this method works only for SFG FROG, because in the higher-order FROG techniques the upconverted peaks at $\tau = T$ do not overlap in the spectral

Table 1. Summary of Capability of Different Pulse Characterization Methods to Determine the Phase Difference Between Well-Separated Components of an Ultrafast Laser Pulse

	Characterization of a Pulse with Components That Are		
Characterization Method	Separated in Time	Separated in Frequency	Separated in Time And Frequency
Spectral Interferometry	Yes	Yes	Yes
Self-referenced FROG (all variants)	Yes[a]	No[b]	No[b]
Self-referenced SPIDER	Yes	No[b]	No[b]
XFROG	Yes	Yes[c]	Yes[c]
XSPIDER	Yes	Yes[c]	Yes[c]
SPC–SFG FROG	Yes	Yes	Yes

[a] Subject to the π or $\pm 2\pi/3$ ambiguity for SHG or THG FROG.
[b] Note that each individual component of the pulse can be fully characterized; only the overall phase difference between components remains undetermined.
[c] The phase of nonequally spaced components can be measured only in a pairwise manner and requires predetermination of the delay and the frequency difference among the components for preparation of the proper reference.

domain. The ultrashort-pulse SPC experiments performed to date[30,31] require a transform-limited pulse with a spectrum spanning the spectrum of the test shaped pulse to create the SPC copy. If such a pulse is available, a simple spectral interferometry experiment will suffice for recovery of the desired information. There are, however, other approaches to creating SPC pulses; these include backward-stimulated Brillouin, Raman, or Rayleigh-wing scattering.[32,33] These methods require no reference pulses and are effectively self-pumped processes. SPC pulses of 20-ps duration have been obtained by use of the stimulated Rayleigh-wing scattering process in a CS_2 cell as the phase-conjugate mirror.[34] If these self-pumped techniques to create spectral phase conjugates can be implemented with sufficient efficiency for complicated ultrashort pulses, a convenient way to characterize multicomponent pulse trains would be provided.

8. CONCLUSIONS

The results of the study reported in this paper are summarized in Table 1. We have demonstrated that, if a laser pulse consists of components that are well separated in the frequency domain, the self-referenced pulse characterization techniques (the pulse spectrum, the autocorrelation, all versions of frequency-resolved optical gating and the spectral phase interferometry for direct electric-field reconstruction), are incapable of yielding the overall phase relation among the spectral components of the pulse. If a well-characterized reference pulse is available, spectral interferometry can determine this phase relation. However, requirements on such a pulse are rather stringent. For cross-correlation FROG these requirements are less stringent, but still a large-bandwidth pulse is needed that has a linear chirp that is determined by the arrival time of the components of the pulse. For a cross-correlation SPIDER, one needs a series of experiments with different spectral shear to obtain the full characterization. In the most general case, if a pulse consists of more than two components that are well separated both in time and in frequency, both for XFROG and XSPIDER the phase difference among the components has to be retrieved in a pairwise manner. We have also outlined an approach that uses sum-frequency mixing of the test pulse with its spectral phase-conjugated copy that is capable, in theory, of recovering the desired phase relation in a single experiment.

APPENDIX A

The description of the pulses [Eq. (2)] used throughout this paper was chosen for mathematical convenience. In this appendix we outline the mathematical relationship of the pulse as described in Eq. (2) to the more-common description of a pulse in which the delay between the components is created through a path-length difference[35]:

$$E(t) = \epsilon_A(t)\exp(-i\omega_A t)\exp(i\phi_A') + \epsilon_B(t - T) \times \exp(-i\omega_B)(t - T)\exp(i\phi_B'); \quad \text{(A1)}$$

in the frequency domain, this becomes

$$\tilde{E}(\omega) = \tilde{\epsilon}_A(\omega - \omega_A)\exp(i\phi_A') + \tilde{\epsilon}_B(\omega - \omega_B) \times \exp[i(\omega - \omega_B)T]\exp(i\phi_B'), \quad \text{(A2)}$$

where the phase of component B at its arrival time $t = T$ is compared to the phase of component A at $t = 0$. One key point about this definition is that phase ϕ_A' of component A is referenced to frequency ω_A, whereas phase ϕ_B' of component B is referenced to ω_B. Because most pulse components do not have a well-defined analytical form (such as a Gaussian profile), the center frequency of a component may be just an arbitrary assignment. Assigning a different frequency as ω_B in an experimentally measured spectrum $\tilde{\epsilon}_B$ in the second term of Eq. (A2) will result in a different ϕ_B'.

This arbitrariness may result in a meaningless definition of phase for which the result of an experiment is the same even though the phase difference as assigned is different. A more meaningful definition of phase that is simpler to define and avoids the phase ambiguities that arise from arbitrary reference frequency assignments can be obtained by comparison of the phase of the electric field of each component to the phase of a reference wave $\exp(i\omega_0 t)$ at the time the component arrives. ω_0 may be

dictated by the experiment and could, for example, correspond to a transition frequency in the system under study.

The phase differences between the two components and this reference depend on time and are, respectively,

$$-\omega_A t + \phi_A' + \omega_0 t, \tag{A3a}$$

$$-\omega_B(t - T) + \phi_B' + \omega_0 t. \tag{A3b}$$

At the arrival time of component A ($t = 0$) this phase difference becomes $\phi_A = \phi_A'$, and for component B at $t = T$ it is $\phi_B = \phi_B' + \omega_0 T$. Using these definitions of the phase in Eq. (A1) yields the expression for the electric field:

$$E(t) = \epsilon_A(t)\exp(-i\omega_A t)\exp(i\phi_A) + \epsilon_B(t - T) \times \exp[i(\omega_B - \omega_0)T]\exp(-i\omega_B t)\exp(i\phi_B). \tag{A4}$$

To avoid making the math in this paper more complex than necessary we have incorporated any additional phase factors introduced by use of a physically meaningful definition of the phase of the components instead of a mathematically convenient one, into the complex field of the pulses; i.e., pulse envelopes $A_A(t)$ and $A_B(t)$ in Eq. (2) are defined as

$$A_A(t) = \epsilon_A(t), \tag{A5a}$$

$$A_B(t - T) = \epsilon_B(t - T)\exp[-i(\omega_B - \omega_0)T]. \tag{A5b}$$

This definition of pulses is also suitable for the description of multicomponent pulses created in a pulse shaper,[1,2] for which no additional path-length-dependent phase in Eq. (A1) is generated.

ACKNOWLEDGMENTS

The authors thank Ian Walmsley for useful discussions and Anthony Miller for his insightful questions. Work at Princeton University was supported by the state of New Jersey and by the U.S. Office of Naval Research; the authors at Georgia Tech acknowledge support from the National Science Foundation.

W. S. Warren's e-mail address is wwarren @princeton.edu.

REFERENCES AND NOTES

1. A. M. Weiner, "Femtosecond pulse shaping using spatial light modulators," Rev. Sci. Instrum. **71**, 1929–1960 (2000).
2. J. X. Tull, M. A. Dugan, and W. S. Warren, "High-resolution, ultrafast laser pulse shaping and its applications," Adv. Magn. Opt. Reson. **20**, 1–65 (1997).
3. R. Trebino, K. W. DeLong, D. N. Fittinghoff, J. N. Sweetser, M. A. Krumbügel, B. A. Richman, and D. J. Kane, "Measuring ultrashort laser pulses in the time-frequency domain using frequency-resolved optical gating," Rev. Sci. Instrum. **68**, 3277–3295 (1997).
4. R. Trebino, *Frequency-Resolved Optical Gating: the Measurement of Ultrashort Laser Pulses* (Kluwer Scientific, Boston, Mass., 2002).
5. C. Iaconis and I. A. Walmsley, "Self-referencing spectral interferometry for measuring ultrashort optical pulses," IEEE J. Quantum Electron. **35**, 501–508 (1999).
6. I. A. Walmsley, "Measuring ultrafast optical pulses using spectral interferometry," Opt. Photonics News **10**(4), 28–33 (1999).
7. X. Gu, L. Xu, M. Kimmel, P. O'Shea, A. P. Shreenath, R. Trebino, and R. S. Windeler, "Frequency-resolved optical gating and single-shot spectral measurements reveal fine structure in microstructure-fiber continuum," Opt. Lett. **27**, 1174–1176 (2002).
8. E. B. Treacy, "Measurement and interpretation of dynamic spectrograms of picosecond light pulses," J. Appl. Phys. **42**, 3848–3858 (1971).
9. J. L. A. Chilla and O. E. Martínez, "Direct determination of the amplitude and the phase of femtosecond light pulses," Opt. Lett. **16**, 39–41 (1991).
10. J.-P. Foing, J.-P. Likforman, M. Joffre, and A. Migus, "Femtosecond pulse phase measurement by spectrally resolved up-conversion: application to continuum compression," IEEE J. Quantum Electron. **28**, 2285–2290 (1992).
11. J.-K. Rhee, T. S. Sosnowski, A.-C. Tien, and T. B. Norris, "Real-time dispersion analyzer of femtosecond laser pulses with use of a spectrally and temporally resolved upconversion technique," J. Opt. Soc. Am. B **13**, 1780–1785 (1996).
12. K. W. Delong, R. Trebino, J. Hunter, and W. E. White, "Frequency-resolved optical gating with the use of 2nd-harmonic generation," J. Opt. Soc. Am. B **11**, 2206–2215 (1994).
13. K. W. DeLong, R. Trebino, and D. J. Kane, "Comparison of ultrashort-pulse frequency-resolved-optical-gating traces for three common beam geometries," J. Opt. Soc. Am. B **11**, 1595–1608 (1994).
14. S. Linden, H. Giessen, and J. Kuhl, "XFROG—A new method for amplitude and phase characterization of weak ultrashort pulses," Phys. Status Solidi B **206**, 119–124 (1998).
15. A. Yabushita, T. Fuji, and T. Kobayashi, "SHG FROG and XFROG methods for phase/intensity characterization of pulses propagated through an absorptive optical medium," Opt. Commun. **198**, 227–232 (2001).
16. D. Keusters, H.-S. Tan, and W. S. Warren, "The failure of nonlinear pulse shape detection," in *Nonlinear Optics*, Vol. 72 of OSA Trends in Optics and Photonics (Optical Society of America, Washington, D.C., 2002), pp. PD3-1–PD3-2.
17. Mode-locked pulse trains have this structure, but we are not considering mode-locked pulse trains here; the short range of relative delays used in most measurements allows for the measurement of only one pulse in such a train, removing the modes from the pulse spectrum.
18. N. F. Scherer, R. J. Carlson, A. Matro, M. Du, A. J. Ruggiero, V. Romerorochin, J. A. Cina, G. R. Fleming, and S. A. Rice, "Fluorescence-detected wave packet interferometry—time resolved molecular spectroscopy with sequences of femtosecond phase-locked pulses," J. Chem. Phys. **95**, 1487–1511 (1991).
19. W. P. de Boeij, M. S. Pshenichnikov, and D. A. Wiersma, "Short-time solvation dynamics probed by phase-locked heterodyne detected pump–probe," Chem. Phys. Lett. **247**, 264–270 (1995).
20. W. P. de Boeij, M. S. Pshenichnikov, and D. A. Wiersma, "Heterodyne-detected stimulated photon echo: applications to optical dynamics in solution," Chem. Phys. Lett. **233**, 287–309 (1998).
21. K. Sundermann and R. de Vivie-Riedle, "Extensions to quantum optimal control algorithms and applications to special problems in state selective molecular dynamics," J. Chem. Phys. **110**, 1896–1904 (1999).
22. D. Zeidler, T. Witte, D. Proch, and M. Motzkus, "Optical parametric amplification of a shaped white-light continuum," Opt. Lett. **26**, 1921–1923 (2001).
23. W. Yang, F. Huang, M. Fetterman, J. Davis, D. Goswami, and W. S. Warren, "Real time adaptive amplitude feedback in an AOM–based ultrafast optical pulse shaping system," IEEE Photonics Technol. Lett. **11**, 1665–1667 (1999).
24. P. J. Delfyett, H. Shi, S. Gee, I. Nitta, J. C. Connolly, and G. A. Alphonse, "Joint time-frequency measurements of mode-locked semiconductor diode lasers and dynamics using fre-

quency resolved optical gating," IEEE J. Quantum Electron. **35**, 487–500 (1999).
25. M. R. Fetterman, J. C. Davis, H.-S. Tan, W. Yang, D. Goswami, J.-K. Rhee, and W. S. Warren, "Fast-frequency-hopping modulation and detection demonstration," J. Opt. Soc. Am. B **18**, 1372–1376 (2001).
26. An example of a pulse with well-separated frequency components whose peaks in the spectrogram do overlap is a three-component pulse, described by

$$E(\omega) = |\tilde{A}_A(\omega - \omega_A)|\exp[i\tilde{\phi}_A(\omega - \omega_A)]\exp(i\phi_A) + |\tilde{A}_B(\omega - \omega_B)|\exp[i\tilde{\phi}_B(\omega - \omega_B)]\exp(i\phi_B) + |\tilde{A}_C(\omega - \omega_C)|\exp[i\tilde{\phi}_C(\omega - \omega_C)]\exp(i\phi_C).$$

The second-harmonic FROG spectrogram of this pulse will have peaks, among others, centered at $\omega_A + \omega_C$ and $2\omega_B$ with phases $\phi_A + \phi_C$ and $2\phi_B$, respectively. When $\omega_A + \omega_C = 2\omega_B$, these two contributions to the peak will beat against each other with fringes dependent on $2\phi_B - (\phi_A + \phi_C)$. If $(\phi_B - \phi_C)$ is known, then $(\phi_B - \phi_A)$ can be deduced and vice versa. This will also be true if components *A* and *C* have a similar delay that is different from that of component *B*.
27. L. Lepetit, G. Chériaux, and M. Joffre, "Linear techniques of phase measurement by femtosecond spectral interferometry for applications in spectroscopy," J. Opt. Soc. Am. B **12**, 2467–2474 (1995).
28. M. Zavelani-Rossi, D. Polli, G. Cerullo, S. De Silvestri, L. Gallmann, G. Steinmeyer, and U. Keller, "Few-optical-cycle laser pulses by OPA: Broadband chirped mirror compressions and SPIDER characterization," Appl. Phys. B **74**, S245–S251 (2002).
29. M. Hirasawa, N. Nakagawa, K. Yamamoto, R. Morita, H. Shigekawa, and M. Yamashita, "Sensitivity improvement of spectral phase interferometry for direct electric-field reconstruction for the characterization of low-intensity femtosecond pulses," Appl. Phys. B **74**, S225–S229 (2002).
30. A. M. Weiner, D. E. Leaird, D. H. Reitze, and E. G. Paek, "Femtosecond spectral holography," IEEE J. Quantum Electron. **28**, 2251–2261 (1992).
31. D. Marom, D. Panasenko, R. Rokitski, P.-C. Sun, and Y. Fainman, "Time reversal of ultrafast waveforms by wave mixing of spectrally decomposed waves," Opt. Lett. **25**, 132–134 (2000).
32. B. Ya. Zel'dovich, N. F. Pilipetsky, and V. V. Shkunov, *Principles of Phase Conjugation* (Springer-Verlag, Berlin, 1985).
33. G. S. He, "Optical phase conjugation: principles, techniques, and applications," Prog. Quantum Electron. **26**, 131–191 (2002).
34. E. J. Miller, M. S. Malcuit, and R. W. Boyd, "Simultaneous wave-front and polarization conjugation of picosecond optical pulses by stimulated Rayleigh-wing scattering," Opt. Lett. **15**, 1188–1190 (1990).
35. A. W. Albrecht, J. D. Hybl, S. M. Gallagher Faeder, and D. M. Jonas, "Experimental distinction between phase shifts and time delays: implications for femtosecond spectroscopy and coherent control of chemical reactions," J. Chem. Phys. **111**, 10,934–10,956 (1999).